

Critical and tricritical behavior in the hierarchical model*

George A. Baker, Jr.

Theoretical Division, University of California, Los Alamos Scientific Laboratory, Los Alamos, New Mexico 87545

Geoffrey R. Golner

Physics Department, University of Washington, Seattle, Washington 98195

(Received 21 December 1976)

The hierarchical model is solved exactly, numerically in the presence of a magnetic and a staggered magnetic field. Critical and tricritical behavior is studied. The general picture of Riedel and Wegner is confirmed. It is shown that their logarithmic corrections are unobservable owing to the interference of higher-order corrections.

I. INTRODUCTION AND SUMMARY

In view of the interest in the study of both critical- and tricritical-point phenomena by methods of the renormalization group, it seemed to us desirable to undertake a study of these phenomena in the context of a model for which the methods of the renormalization group can be applied without approximation. For the hierarchical model,^{1,2} the exact solution can be obtained by the numerical iteration of certain nonlinear integral recursion relations. If the lattice spins are distributed according to the law $\exp(as^2 - bs^4)$ ($b > 0$), and the fundamental exchange energy is of ferromagnetic sign, then^{1,3} all the usual theorems and inequalities of the ferromagnetic Ising model hold. Since the critical indices for this model are nontrivial, it thus seems to us to be a likely place to investigate the sort of critical and tricritical behavior which can occur in the framework of renormalization-group theory.

We found that the general picture of behavior near the critical and the tricritical points as developed by Riedel and Wegner^{4,5} is correct. However, the logarithmic corrections which they predict at four-dimensional critical and three-dimensional tricritical points cannot be experimentally observed because of the strong and *very slowly decaying* corrections to leading-order behavior. Another point of practical significance, both for theoretical analysis and the analysis of experimental data, relates to the accuracy of the location of the tricritical point. Although we were able to locate an ordinary critical point to full machine accuracy (about 14 figures), the additional fluctuations associated with the tricritical point reduced our accuracy to about half that for the critical point.

In the second section, we review some of the elementary theory of the hierarchical model with emphasis on the inclusion of both magnetic and stag-

gered magnetic fields. We also indicate how the Blume-Emery-Griffiths model⁶ can be studied as a hierarchical model in a staggered field. The Wilson⁷ approximate renormalization-group recursion formula is discussed and is shown to be, as is also the hierarchical model, a special case of the Wilson-Fisher⁸ generalized approximate renormalization-group recursion formula.

In Sec. III, we discuss in some detail the behavior of the solutions of the recursion relations near the critical point. We describe the behavior at $T < T_c$ where a spontaneous magnetization can occur, at $T = T_c$ where there is convergence to a fixed-point solution and at $T > T_c$ where there is no spontaneous magnetization and the magnetic susceptibility is finite. We are able to compute the curves of the critical exponents $\gamma(\sigma/d)$ and $\beta(\sigma/d)$. The quantity σ is a parameter [see (2.1)] determining the behavior of the interaction and d is the spatial dimension. These results are compared with the ϵ expansion⁹ and the known results for the spin- $\frac{1}{2}$ Ising model. We compute the susceptibility and magnetization for $\sigma/d = \frac{1}{2}$ in order to display the logarithmic corrections. The apparent results are at variance with the predictions of Wegner and Riedel⁵ and we attribute this difference to corrections to the leading-order behavior.

In the last section, we discuss the behavior near the tricritical point. We find second-order critical points, a tricritical point, first-order transition points, and wings bounded by second-order wing critical points. All these are much as expected. We present results for $\sigma/d = \frac{3}{5}$, $\frac{2}{3}$, and $\frac{7}{8}$ which show classical tricritical exponents, classical exponents with logarithmic corrections, and nonclassical exponents, respectively. The plots of magnetization, as a function of temperature with the other parameters held fixed, and the magnetization along the first-order line, show logarithmic corrections which apparently differ from those predicted. We again attribute these differences to higher-order corrections.

II. HIERARCHICAL MODEL

The model we study has been discussed in detail in Ref. 1. Here, we present a brief review with attention on the effects of the external fields, which we now incorporate in the model.

We first discuss the model in one dimension. The model consists of a system of $N = 2^L$ interacting spins $\{\nu_j\}$, described by the Hamiltonian

$$\mathcal{H} = J \sum_{\mu=0}^{L-1} 2^{-\mu\sigma} \sum_{m=1}^{2^{L-1-\mu}} S_{m,\mu}^2 - \frac{1}{2} J \left(\frac{1 - 2^{-L(1+\sigma)}}{1 - 2^{-1-\sigma}} \right) \sum_{j=1}^{2^L} \nu_j^2 + \bar{m} H' \sum_{j=1}^{2^L} (-1)^{j-1} \nu_j + \bar{m} H \sum_{j=1}^{2^L} \nu_j, \quad (2.1)$$

where

$$S_{m,\mu+1} = \frac{(\hat{S}_{2m-1,\mu} - \hat{S}_{2m,\mu})}{\sqrt{2}},$$

$$\hat{S}_{m,\mu+1} = \frac{(\hat{S}_{2m-1,\mu} + \hat{S}_{2m,\mu})}{\sqrt{2}}, \quad (m = 1, \dots, 2^{L-2-\mu}),$$

$$\hat{S}_{j,-1} = \nu_j \quad (j = 1, \dots, 2^L),$$
(2.2)

for $\mu = -1, 0, 1, \dots, L-2$. The first two terms in the Hamiltonian describe the interaction between spins according to the hierarchy of spin groupings as shown in Fig. 1. We see that each spin interacts with every other spin beginning at some level l of the hierarchy. In terms of this level l we can write the spin-spin interaction as

$$\frac{-J \nu_j \nu_{j'}}{2^{l(\sigma+1)}} \left(\frac{2^{\sigma+1} - 2}{2^{\sigma+1} - 1} \right) \quad (2.3)$$

(in the limit $L \rightarrow \infty$). For $J > 0$ we therefore have a long-range ferromagnetic interaction decaying in a stair step fashion roughly as $r^{-1-\sigma}$.

The remaining terms in the Hamiltonian involving H and H' represent, respectively, the uniform and staggered applied fields which couple to the spins ν_j via their magnetic moments \bar{m} . For ferromagnetic coupling, $J > 0$, we see that the uniform field couples to the order parameter, and hence the coupling can be written in terms of the mean spin

$$\bar{m} H \sum_{j=1}^{2^L} \nu_j = \bar{m} H N^{1/2} \hat{S}_{1,L-1}. \quad (2.4)$$

The coupling to the staggered field can also be written

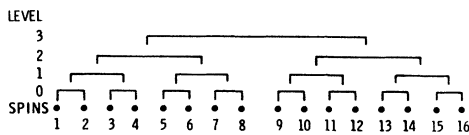


FIG. 1. The spin-grouping hierarchy used for our one-dimensional model.

$$\bar{m} H' \sum_{j=1}^{2^L} (-1)^{j-1} \nu_j = \bar{m} H' \sum_{m=1}^{2^{L-2}} \sqrt{2} S_{m,0}. \quad (2.5)$$

The partition function for this system can be written

$$Z = \prod_j \left(\int_{-\infty}^{\infty} d\nu_j U(\nu_j) \right) e^{\beta \mathcal{H}}, \quad (2.6)$$

where $U(\nu_j)$ represents a spin-weight probability distribution for the ν_j , which can be chosen to interpolate between the continuous-spin, Gaussian, and fixed-length-spin, Ising models. The standard form that we use for $U(\nu)$ is

$$U(\nu) = e^{-\frac{1}{2}(a\nu^2 + b\nu^4)} \quad (a < 0, b > 0). \quad (2.7)$$

It is convenient to define the function $P(\nu)$ by the relation

$$U(\nu) = \exp \left[-\frac{1}{2} K \left(\frac{1 - 2^{-L(1+\sigma)}}{1 - 2^{-1-\sigma}} \right) \nu^2 - \frac{1}{2} P(\nu) \right], \quad (2.8)$$

where $K = \beta J$. So,

$$P(\nu) = \left[a - K \left(\frac{1 - 2^{-L(1+\sigma)}}{1 - 2^{-1-\sigma}} \right) \right] \nu^2 + b \nu^4. \quad (2.9)$$

Using the spin transformations of Eq. (2.2), we can write the partition function, following Ref. 1, as

$$Z = \prod_{\mu=0}^{L-1} \left[2^{\sigma/2} \sqrt{K} I_{\mu}(0) 2^{L-1-\mu} \right] \times \int_{-\infty}^{\infty} \exp \left[\beta \bar{m} H \times 2^{L/2} \hat{S}_{1,L-1} - \frac{1}{2} Q_L \right] \times \left(\frac{(2K)^{1/2} \hat{S}_{1,L-1}}{2^{\sigma L/2}} \right) \frac{d\hat{S}_{1,L-1}}{2^{\sigma L/2}} \quad (2.10)$$

where $Q_L(x)$ is determined via the recursion relation

$$Q_{\mu+1}(x) = -2 \ln [I_{\mu}(2^{-(1-\sigma)/2} x) / I_{\mu}(0)], \quad (2.11)$$

where

$$I_{\mu}(x) = \int_{-\infty}^{\infty} dy \exp \left[-y^2 - \frac{1}{2} Q_{\mu}(x+y) - \frac{1}{2} Q_{\mu}(x-y) \right], \quad \mu > 0 \quad (2.12)$$

and

$$I_0(x) = \int_{-\infty}^{\infty} dy \exp \left[-y^2 + \beta \bar{m} H' (2/K)^{1/2} y - \frac{1}{2} Q_0(x+y) - \frac{1}{2} Q_0(x-y) \right] \quad (2.13)$$

with $Q_0(y) \equiv P((2K)^{-1/2} y)$. The term $\beta \bar{m} H' (2/K)^{1/2} y$ in the equation for $I_0(x)$ is due to the presence of the staggered magnetic field, which, as we recall from Eq. (2.5) above, is coupled to the variables $S_{m,0}$ which are integrated out at the first level of the hierarchy. Note that in contrast to the earlier

treatment of Ref. 1 we have incorporated K into the definition of Q_0 so that it does not appear in the recursion formulas Eqs. (2.11) and (2.12).

Looking at our expression for the partition function, Eq. (2.10), we see that it is particularly well suited for the calculation of thermodynamic func-

tions associated with the order parameter, as the order parameter is the last variable remaining to be integrated, and all H dependence appears explicitly. We therefore obtain the following simple expressions for the uniform magnetization M and uniform susceptibility χ

$$M = - \frac{\partial(\ln Z)}{\partial(\beta H)} = \bar{m} N^{1/2} \frac{\int_{-\infty}^{\infty} S_{1,L-1} \exp\{-\frac{1}{2} W_L((2K)^{1/2} 2^{-\sigma L/2} \hat{S}_{1,L-1})\} d\hat{S}_{1,L-1}}{\int_{-\infty}^{\infty} \exp\{-\frac{1}{2} W_L((2K)^{1/2} 2^{-\sigma L/2} \hat{S}_{1,L-1})\} d\hat{S}_{1,L-1}}, \quad (2.14)$$

$$\chi = \frac{\partial M}{\partial H} - \beta M^2 = \bar{m}^2 \beta N \frac{\int_{-\infty}^{\infty} (\hat{S}_{1,L-1})^2 \exp\{-\frac{1}{2} W_L((2K)^{1/2} 2^{-\sigma L/2} \hat{S}_{1,L-1})\} d\hat{S}_{1,L-1}}{\int_{-\infty}^{\infty} \exp\{-\frac{1}{2} W_L((2K)^{1/2} 2^{-\sigma L/2} \hat{S}_{1,L-1})\} d\hat{S}_{1,L-1}}, \quad (2.15)$$

where

$$\exp\{-\frac{1}{2} W_L((2K)^{1/2} 2^{-\sigma L/2} \hat{S}_{1,L-1})\} = \exp\{\bar{m} H \beta N^{1/2} \hat{S}_{1,L-1} - \frac{1}{2} Q_L((2K)^{1/2} 2^{-\sigma L/2} \hat{S}_{1,L-1})\} \quad (2.16)$$

is seen to represent the order parameter probability distribution for the N spin system at the last level of the hierarchy. Thus the critical behavior of M and χ can be determined quite straightforwardly.

The calculation of the thermodynamic functions associated with the staggered order parameter is more complicated, since the staggered order parameter is integrated out at the lowest level of the hierarchy, and therefore the H' dependence of Eq. (2.10) does not appear explicitly, but rather is implicitly contained in the quantities $I_\mu(0)$ and $Q_L(x)$ which appear in the expression for Z . A similar difficulty is encountered in the calculation of the specific heat. These quantities must therefore be calculated directly from the expression for the free energy per spin

$$\begin{aligned} \frac{F}{N} = & -kT \left(1 - \frac{1}{N}\right) \sigma \ln 2 - kT \sum_{\mu=0}^{L-1} 2^{-1-\mu} \ln[I_\mu(0)] \\ & - \frac{kT}{N} \ln \int_{-\infty}^{\infty} \exp\left[-\frac{1}{2} Q_L((2K)^{1/2} 2^{-\sigma L/2} S_{1,L-1})\right] \\ & \times \frac{d\hat{S}_{1,L-1}}{2^{\sigma L/2}} \end{aligned} \quad (2.17)$$

which sums contributions from each level of the hierarchy. The calculation of these quantities will not be discussed further here. The remainder of this paper will be concerned only with the behavior of the order parameter, which can be studied directly via the distribution function $W_L(x)$.

Though so far, our discussion has concerned ordering of a system with long-range ferromagnetic interactions, it is useful to observe that our discussion applies, with the appropriate symmetry arguments, to a system that orders antiferromagnetically. That is, the Hamiltonian will be un-

changed if we change the sign of every other spin (even numbered) and at the same time change every odd-neighbor interaction (first nearest, third nearest, etc.) from ferromagnetic to antiferromagnetic. This symmetry is further manifest by the recursion formulas if we define the new transformed set of variables:

$$t_{m,\mu+1} = (\hat{t}_{2m-1,\mu} - \hat{t}_{2m,\mu})/\sqrt{2}, \quad (2.18)$$

$$\hat{t}_{m,\mu+1} = (\hat{t}_{2m-1,\mu} + \hat{t}_{2m,\mu})/\sqrt{2} \quad (m=1, \dots, 2^{L-2-\mu})$$

for $\mu=0, 1, \dots, L-2$ as before, and

$$t_{m,0} = (\nu_{2m-1} + \nu_{2m})/\sqrt{2}, \quad (2.19)$$

$$\hat{t}_{m,0} = (\nu_{2m-1} - \nu_{2m})/\sqrt{2} \quad (m=1, \dots, 2^{L-1}),$$

which is new. In terms of these new variables we can write the new Hamiltonian

$$\begin{aligned} \mathcal{H} = & J \sum_{\mu=0}^{L-1} 2^{-\mu\sigma} \sum_{m=1}^{2^{L-1-\mu}} t_{m,\mu}^2 - \frac{1}{2} J \left(\frac{1 - 2^{-L(1+\sigma)}}{1 - 2^{-1-\sigma}} \right) \sum_{j=1}^L \nu_j^2 \\ & + \bar{m} H' N^{1/2} \hat{t}_{1,L-1} + \bar{m} H \sum_{m=1}^{2^{L-2}} \sqrt{2} t_{m,0} \end{aligned} \quad (2.20)$$

which has the desired long-range, spin-spin interaction (in the thermodynamic limit)

$$-\frac{J(-1)^{i-j} \nu_i \nu_j}{2^{j(\sigma+1)}} \left(\frac{2^{\sigma+1} - 2}{2^{\sigma+1} - 1} \right). \quad (2.21)$$

By comparing this Hamiltonian with the ferromagnetic Hamiltonian of Eqs. (2.1), (2.4), and (2.5), we see that while the staggered and uniform order parameters have exchanged roles, the equation for the partition function with the associated recursion formulas, Eqs. (2.11) and (2.12), is otherwise unchanged. Thus in each case the renormalization-

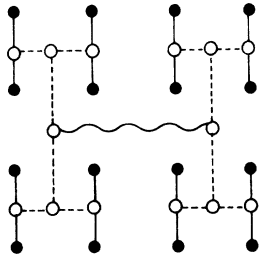


FIG. 2. "H-model", a grouping of a two-dimensional lattice of spins which is structurally equivalent to Fig. 1.

group recursion relations behave identically once they are defined in terms of the appropriate order parameter.

All of the above discussion can be easily generalized to a system of $N = 2^{Ld}$ spins in d dimensions according to the arrangement shown in Fig. 2. If, in the above equations, we make the replacements $L \rightarrow Ld$ and $\sigma \rightarrow \sigma/d$, we then have the equations appropriate for describing the spin system of Fig. 2 with long-range, spin-spin interaction

$$\frac{-J\nu_i\nu_j}{2^{L(\sigma+d)/d}} \left(\frac{2^{\sigma/d+1} - 2}{2^{\sigma/d+1} - 1} \right). \quad (2.22)$$

Thus, if we approximate $r \approx 2^{1/d}$, we see that we have a long-range interaction decaying in a stair step fashion approximately as $r^{-d-\sigma}$. Following the discussion above it is again trivial to show the equivalence of ferroferromagnetic, meta-ferromagnetic, and antiferromagnetic systems. In d dimensions, the first d -level equations of the hierarchy will then differ from the rest. The asymptotic structure remains again the same as in the ferromagnetic case.

In addition to the H -model extension to higher dimensions, Baker¹ also introduced a different extension. The two-dimensional version or planar model is illustrated in Fig. 3. This model is more difficult to study numerically than the H -model since it requires a $(2^d - 1)$ -dimensional integration at each iteration step rather than a one-dimensional one. So far as we know, it has only been investigated numerically by Furman,¹⁰ and he did the two-dimensional case. Furman has shown an equivalence relation. If the spins in a fundamental square of the hierarchy interact as

$$\begin{aligned} E = & K \left(\alpha^2 - \frac{1}{4} \right) (\nu_{1,1} - \nu_{1,2})^2 + \frac{1}{4} (\nu_{1,2} - \nu_{2,2})^2 \\ & + (\alpha^2 - \frac{1}{4}) (\nu_{2,1} - \nu_{2,2})^2 + \frac{1}{4} (\nu_{1,1} - \nu_{2,1})^2 \\ & + \frac{1}{4} (\nu_{1,1} - \nu_{2,2})^2 + \frac{1}{4} (\nu_{1,2} - \nu_{2,1})^2 \\ & - \left(\frac{1}{4} + \alpha^2 \right) \sum_{i,j=1}^2 \nu_{i,j}^2, \end{aligned} \quad (2.23)$$

where $\frac{1}{2} \leq \alpha^2 \leq 1/\sqrt{2}$, then the formulas for the

planar model are just the same as a double iteration of the H model where $\alpha^2 = 2^{-(1+\eta/d)/2}$. If the planar model has universality, then its results could be inferred from the special case of the H model. Furman partially checked this hypothesis and found agreement at the one point he checked. That is to say, he found $\gamma = 1.300 \pm 0.005$ for the planar model versus $\gamma = 1.2991$ for the corresponding H -model result.

The renormalization-group studies by Riedel and Wegner of tricritical behavior in the Blume-Emery-Griffiths⁶ model provide a valuable guide for our expectations for the hierarchical model. To see this, we recall that the Wilson approximate renormalization-group recursion formula used by Riedel and Wegner,⁴ in their study, has been shown by Baker¹ to be, in some sense, exact for the hierarchical model. Thus, if the model Hamiltonians for the two systems can be shown to belong to the same universality class, we can expect that the systems will exhibit quantitatively similar critical behavior. Since, at first glance, the model Hamiltonians for the two systems appear quite dissimilar, it is a useful exercise to demonstrate how they can become equivalent in a renormalization-group context.

To study the Blume-Emery-Griffiths model using Wilson's approximate renormalization-group recursion formula⁷ Riedel and Wegner⁴ first transformed the original spin-one Hamiltonian to a Landau-Ginsburg form

$$\mathcal{H} = -K \int_x [\vec{\nabla} S(x)]^2 - \int_x P(S(x)), \quad (2.24)$$

where the function $P(S(\vec{x}))$ is chosen in order that $\exp[-\int_x P(S(x))]$ represents a continuous-spin, probability distribution which mimics a spin-one system. This mimicry will be the case if we choose $P(S(x))$ to have the form

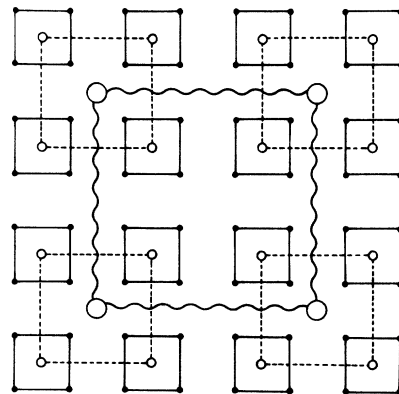


FIG. 3. The spin grouping hierarchy used for our planar model.

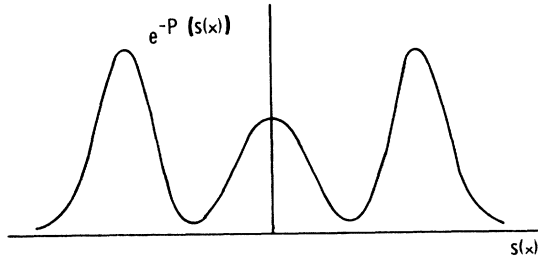


FIG. 4. A continuous spin-probability distribution which mimics a discrete $s=1$ case.

$$P(S(\vec{x})) = A[S(\vec{x})]^2 - B[S(\vec{x})]^4 + C[S(\vec{x})]^6 \quad (2.25)$$

with $A, B, C > 0$, in which case $\exp[-\int_{\vec{x}} P(S(\vec{x}))]$ will have the form shown in Fig. 4. We recall that after writing $P(S(\vec{x}))$ in an appropriately rescaled form as

$$Q_0(y) = A'y^2 - B'y^4 + C'y^6 \quad (2.26)$$

it will transform according to the Wilson-Fisher generalization⁸ of Wilson's approximate renormalization group recursion formula⁷ as

$$Q_{\mu+1}(y) = -b^d \ln[I_{\mu}(b^{(1-d/2)}y)/I_{\mu}(0)], \quad (2.27)$$

where

$$I_{\mu}(y) = \int_{-\infty}^{\infty} dx \exp[-x^2 - \frac{1}{2}Q_{\mu}(y+x) - \frac{1}{2}Q_{\mu}(y-x)]. \quad (2.28)$$

The parameter b in the above equation is related to the change in momentum space cutoff accomplished by the renormalization-group transformation: i.e., after μ iterations of the renormalization group the momentum range for the Fourier transformed effective Hamiltonian is $0 \leq |k| \leq b^{-\mu}$. We see that if b is chosen $b = 2^{1/d}$ then the recursion formula of Wilson-Fisher is identical to that of the H -configuration hierarchical model with σ set equal to 2. If $b = 2$, then the original Wilson approximate renormalization-group recursion formula is obtained.

In the Riedel and Wegner analysis, the nonordering field is coupled to the system described by Eq. (2.26) via the coefficient A' , which also depends linearly on the temperature. For values of A' less than, equal to, or greater than its tricritical value A'_t , the system underwent critical, tricritical, and first-order transitions, respectively.

In the case of the hierarchical model the nonordering, staggered magnetic field appears first in Eq. (2.13) for $I_0(x)$, instead of $Q_0(x)$, as in the Riedel and Wegner analysis. However, after one iteration of the recursion formula the structure of the nonordering field dependence becomes the same in the two models. To show this result, we start

from the standard continuous spin- $\frac{1}{2}$, Ising distribution function

$$Q_0(x) = r_0 x^2 + \lambda_0 x^4, \quad (2.29)$$

and compute $Q_1(x)$ to second order in λ_0 using Eqs. (2.11) and (2.13). We find, to order λ_0^2 , for $\sigma = 2$,

$$Q_1(x) = r_1 x^2 + \lambda_1 x^4, \quad (2.30)$$

with

$$r_1 = 2^{2/d} \left[r_0 + \frac{3\lambda_0}{1+r_0} (1+2h^2) - \frac{\lambda_0^2}{(1+r_0)^3} (9+54h^2+24h^4) \right], \quad (2.31)$$

$$\lambda_1 = 2^{(4-d)/d} \left[\lambda_0 - \frac{\lambda_0^2}{(1+r_0)^2} (9+36h^2) \right],$$

where $h \equiv \beta \bar{m} H' / [2K(1+r_0)]^{1/2}$. We now see a qualitative similarity between this system (after one iteration) and the system described by Eq. (2.24), as now the nonordering field couples directly to the quadratic and quartic terms. We see, in fact, that for large enough values of h , the coefficient λ_1 can become negative, while r_1 can become positive, thereby resulting in a spin probability distribution $e^{-Q_1(y)}$ of the same form as that in Fig. 4 which was used in the Riedel-Wegner⁴ analysis of the Blume-Emery-Griffiths⁶ model. The asymptotic analysis of the Q functions for large values of the argument indicates that it becomes large and positive. Therefore, there must be higher-order terms present to insure this behavior. Riedel and Wegner have chosen the simplest such, i.e., an x^6 term. Thus, we may reasonably expect that the hierarchical model in large enough nonordering staggered field will have the same tricritical behavior as that of the Blume-Emery-Griffiths model.

The analysis of Wegner and Riedel^{4,5} directly predicts that this model will have a Gaussian critical point in four dimensions with logarithmic corrections and that the susceptibility will behave as ($\tau = T_c - T$)

$$\chi \propto |\tau|^{-1} |\ln|\tau||^{1/3} \quad (2.32)$$

there, and that the spontaneous magnetization will behave as

$$M \propto |\tau|^{1/2} |\ln|\tau||^{1/3} \quad (2.33)$$

which results agree with those obtained by Larkin and Khmel'nitskii¹¹ from diagrammatic techniques. The same results can be obtained directly in the context of the Callan-Symanzik equation as was shown by Brézin *et al.*⁹ The Callan-Symanzik equation is thought to be relevant to the Landau-Ginzberg Hamiltonian rather than to the Wilson approximate recursion relations.

In addition, Wegner and Riedel find that the tri-

critical point for the model three dimensions is of the Gaussian type, but with logarithmic corrections. Specifically they predict that ($\tau = T_t - T$)

$$\chi_t \propto |\tau|^{-1}, M_t \propto |\tau|^{1/4} |\ln|\tau||^{1/4}, \quad (2.34)$$

for the temperature near the tricritical temperature, the staggered field fixed at its tricritical value and the magnetic field fixed at zero. For the behavior of the magnetization along the first-order line near the tricritical point

$$M_1 \propto |\tau|^{1/2} |\ln|\tau||^{7/10}. \quad (2.35)$$

They, however, emphasize that their analysis ignores correction terms of the order $|\ln|\tau||^{-1/2}$ smaller than the leading order. Since $\ln|\tau|$ varies rather slowly over the experimental range, it is not especially clear whether the leading logarithmic corrections are experimentally accessible or not. An alternative calculation by diagrammatic methods of the logarithmic corrections has been given by Stephen *et al.*¹² with a slightly different form of the free energy.

One important property found by Riedel and

Wegner is that although the coefficients, and presumably the corrections to the leading order behavior, depend on the parameter b [see Eq. (2.27)], the critical exponents and the logarithmic corrections do not. Thus, their results should be equally valid for the Baker hierarchical model and the Wilson approximate renormalization-group recursion relations.

III. NUMERICAL RESULTS NEAR THE CRITICAL POINTS

In this section, we will discuss how calculational procedures can be used to derive information about the behavior of the thermodynamic functions near a critical point of the hierarchical model. We will give some of the results we have obtained for both this model and for Wilson's approximate renormalization-group recursion relations.⁷

First we may obtain computationally convenient expressions for the magnetization and the susceptibility. Using Eq. (2.10) for the partition function we can write

$$M = \frac{\partial F}{\partial H} = \bar{m} N^{1/2} \left(\int_{-\infty}^{+\infty} \hat{S}_{1, Ld-1} \exp\left\{-\frac{1}{2} W_{Ld} \left((2K)^{1/2} \hat{S}_{1, Ld-1} / 2^{\sigma L/2} \right)\right\} d\hat{S}_{1, Ld-1} \right) \times \left(\int_{-\infty}^{+\infty} \exp\left\{-\frac{1}{2} W_{Ld} \left((2K)^{1/2} \hat{S}_{1, Ld-1} / 2^{\sigma L/2} \right)\right\} d\hat{S}_{1, Ld-1} \right)^{-1}, \quad (3.1)$$

$$\chi = \frac{\partial M}{\partial H} = \bar{m}^2 \beta N \left(\int_{-\infty}^{+\infty} (\hat{S}_{1, Ld-1})^2 \exp\left\{-\frac{1}{2} W_{Ld} \left((2K)^{1/2} \hat{S}_{1, Ld-1} / 2^{\sigma L/2} \right)\right\} d\hat{S}_{1, Ld-1} \right) \times \left(\int_{-\infty}^{+\infty} \exp\left\{-\frac{1}{2} W_{Ld} \left((2K)^{1/2} \hat{S}_{1, Ld-1} / 2^{\sigma L/2} \right)\right\} d\hat{S}_{1, Ld-1} \right)^{-1} - \beta M^2, \quad (3.2)$$

where

$$\exp\left\{-\frac{1}{2} W_{Ld} \left((2K)^{1/2} \hat{S}_{1, Ld-1} / 2^{\sigma L/2} \right)\right\} = \exp\left\{\bar{m} H \beta N^{1/2} \hat{S}_{1, Ld-1} - \frac{1}{2} Q_{Ld} \left((2K)^{1/2} \hat{S}_{1, Ld-1} / 2^{\sigma L/2} \right)\right\} \quad (3.3)$$

is seen to represent the order parameter ($\hat{S}_{1, Ld-1}$) probability distribution for the $N = 2^{Ld}$ spin system at the last level of the hierarchy. If we consider the system in the thermodynamic limit $L \rightarrow \infty$, we find that for $Ld \gg \xi$, the correlation length, the distribution function $\hat{W}_{Ld}(x)$ has a simple limiting behavior when transformed back to the original lattice scale.^{2,13} If we write

$$U_\mu(x) = 2^{-\mu} W_\mu \left((2K)^{1/2} 2^{\mu(d-\sigma)/2} x \right), \quad (3.4)$$

$$S_{1, \mu-1} = 2^{\mu/2} z = N_\mu^{1/2} z, \quad (3.5)$$

then the equation for the magnetization becomes

$$M_\mu = \bar{m} N_\mu \left(\int_{-\infty}^{+\infty} z \exp\left[-\frac{1}{2} N_\mu U_\mu(z)\right] dz \right) \times \left(\int_{-\infty}^{+\infty} \exp\left[-\frac{1}{2} N_\mu U_\mu(z)\right] dz \right). \quad (3.6)$$

If we assume that U_μ has a minimum at $z = z_{0, \mu}$ and can be expanded about that point so that

$$U_\mu(z) = U_\mu(z_{0, \mu}) + \frac{1}{2} U_\mu''(z_{0, \mu})(z - z_{0, \mu})^2 + \dots \quad (3.7)$$

then, by the saddle-point approximation (3.6) becomes [N large and $U_\mu''(z_0)$ finite]

$$M_\mu = \bar{m} N_\mu \left(\int_{-\infty}^{+\infty} z \exp\left[-\frac{1}{4} N_\mu U_\mu''(z_{0, \mu})(z - z_{0, \mu})^2\right] dz \right) \times \left(\int_{-\infty}^{+\infty} \exp\left[-\frac{1}{4} N_\mu U_\mu''(z_{0, \mu})(z - z_{0, \mu})^2\right] dz \right)^{-1} = \bar{m} N_\mu z_{0, \mu} = (\bar{m} N / 2\sqrt{K}) 2^{-\mu(1-\sigma/d)/2} y_{0, \mu}. \quad (3.8)$$

Similarly, it is straightforward to compute from (3.2) that

$$\begin{aligned}\chi &= 2\bar{m}^2\beta N/U_\mu''(z_{0,\mu}), \\ &= \bar{m}^2 N 2^{\mu\sigma/d} / [JW_\mu''(y_{0,\mu})],\end{aligned}\quad (3.9)$$

where

$$y_{0,\mu} = (2K)^{1/2} 2^{\mu(d-\sigma)/2d} z_{0,\mu} \quad (3.10)$$

is on the scale of the argument of the Q and W functions.

With these preliminaries we are in a position to investigate the critical behavior by numerically integrating the recursion formulas, Eqs. (2.11) and (2.12) for the hierarchical model and Eqs. (2.27) and (2.28) with $b = 2$ for Wilson's equation.

We describe briefly our numerical procedure: The function $Q_\mu(x)$ was calculated on a uniformly spaced mesh of points over a domain whose size was allowed to vary so as to include the range $Q_\mu(x) < 300$. The mesh spacing Δ was chosen to be $\Delta = 0.025$ for the studies of ordinary critical points, and $\Delta = 0.1$ for the studies of tricritical and wing critical points. Integrals such as Eqs. (2.12) and (2.13) were calculated using a five-point Newton-Cotes formula,¹⁴ with error term typically of order Δ^7 . New values of $Q_{\mu+1}(x)$ were interpolated, as in Eq. (2.11), using five-point Lagrange interpolation,¹⁵ with an error typically of order $10^{-2}\Delta^5$.

In the hierarchical model, the spin distribution of Eq. (2.7) was chosen with a and b fixed, typically at $a = -0.5$ and $b = 0.1$. The initial rescaled distribution function $Q_0(y)$ then varied with temperature ($K = \beta J$) as

$$Q_0(y) = \frac{1}{2} \left[\frac{a}{K} - \frac{1}{1 - 2^{(\sigma-d)/d}} \right] y^2 + \frac{b}{4K^2} y^4, \quad (3.11)$$

where we have taken the $\lim L \rightarrow \infty$ in the first term. The critical fixed point was found by varying the input value of K and observing the qualitatively different behavior of the iterated function $Q_\mu(y)$ depending on whether K was chosen greater than,

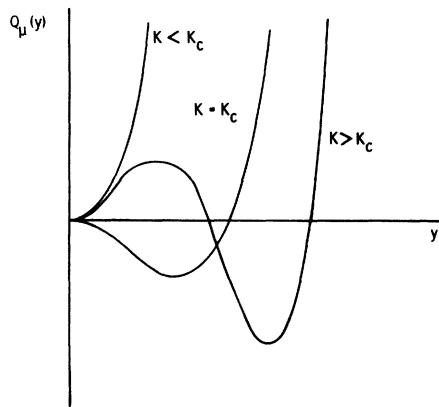


FIG. 5. Qualitative, large μ , behavior of the iterated function $Q_\mu(y)$ in the regions $K < K_c$, $K = K_c$, and $K > K_c$.

TABLE I. Iterations for the case $\sigma/d = 0.55$ and $K - K_c = 10^{-6}$.

| μ | M | χ |
|-------|-----------|----------|
| 1 | 1.629 7 | 0.220 43 |
| 10 | 0.453 79 | 38.414 |
| 20 | 0.097 678 | 288.37 |
| 30 | 0.024 318 | 115 984 |
| 35 | 0.017 276 | 319 005 |
| 40 | 0.016 107 | 421 846 |
| 41 | 0.016 069 | 427 161 |
| 42 | 0.016 049 | 430 209 |
| 43 | 0.016 038 | 431 879 |
| 44 | 0.016 032 | 432 770 |
| 45 | 0.016 029 | 433 235 |
| 46 | 0.016 028 | 433 473 |

equal to, or less than K_c , its critical value (see Fig. 5). By successively refining the input value, the critical value of $K = K_c$ could thus be determined to the numerical precision of the computer.

Once the critical point was found, the magnetization and susceptibility could be calculated for noncritical values of K by iterating the recursion formula until $2^{\mu/d}$ becomes large compared to the correlation length, at which point the Eqs. (3.8) and (3.9) approach their limiting values for M and χ .^{2,13} An example is illustrated in Table I, where we have listed values of the magnetization M , and susceptibility χ , calculated from Eqs. (3.8) and (3.9) for values of $2^{\mu/d}$ exceeding the correlation length. If we write Eq. (3.9) for χ as

$$W_\mu''(y_0) = (\bar{m}^2 N / J\chi) 2^{\mu\sigma/d}, \quad (3.12)$$

we see that the spin distribution function $e^{-W_\mu(y)/2}$ becomes more and more narrowly peaked about its maximum value $e^{-W_\mu(y_0)/2}$, indicating the exponential decrease of spin fluctuations once the recursion formulas have been iterated beyond the correlation length. This behavior of the function $W_\mu(y)$ is shown qualitatively in Figs. 6 and 7 for $K < K_c$.

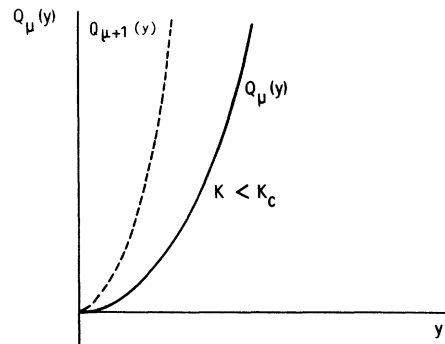


FIG. 6. Qualitative, large μ , behavior of the function $Q_\mu(y)$ under successive iteration in the region $K < K_c$.

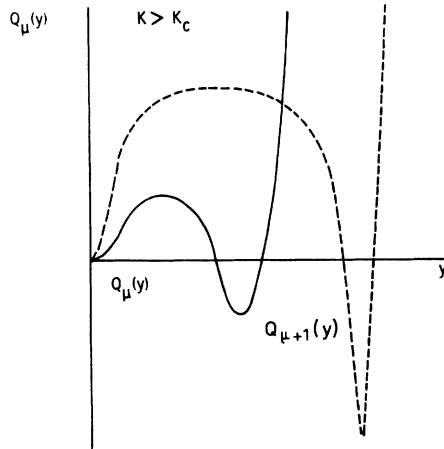


FIG. 7. Qualitative, large μ , behavior of the function $Q_\mu(y)$ under successive iteration in the region $K > K_c$.

and $K > K_c$, respectively. This particular example was calculated for the Ising model, $\sigma/d = 0.55$, $K_c - K = 10^{-6}$. We see that, as the number of iterations increases, both M and χ appear to be converging to their limiting values. Based on the values in Table I, we estimate the limiting values to be $M = 0.016\,02 \pm 0.000\,01$ and $\chi = (4.34 \pm 0.01) \times 10^5$. This example is typical of all our results.

The recursion relations [Eqs. (2.11) and (2.12)] were first studied in zero external field to determine the critical behavior as a function of the ratio σ/d . Since there is no transition in the model for $\sigma/d > 1$, and the transition becomes Gaussian for $\sigma/d \leq \frac{1}{2}$, the interesting range of study is $\frac{1}{2} \leq \sigma/d < 1$. Starting with an initial spin probability distribution corresponding to $a = -0.5$ and $b = 0.1$ in Eq. (2.7), the critical values of K_c were determined for the values σ/d as given in Table II. The magnetization and susceptibility values were then calculated for a range of K values, $10^{-6} \leq K - K_c \leq 1$, for each σ/d , from which the critical exponents β and $\gamma' (= \gamma)$ were obtained. Magnetization and susceptibility curves for

TABLE II. Critical-point parameters for the hierarchical model.

| σ/d | K_c | γ' | β |
|---------------|--------------|-----------|---------|
| 0.50 | 0.299 820 37 | 1.000 | 0.500 |
| 0.55 | 0.313 666 90 | 1.073 | 0.439 |
| 0.60 | 0.328 550 54 | 1.157 | 0.386 |
| $\frac{2}{3}$ | 0.350 206 40 | 1.299 | 0.325 |
| 0.72 | 0.369 281 44 | 1.440 | 0.280 |
| 0.77 | 0.388 913 99 | 1.607 | 0.240 |
| 0.82 | 0.410 749 53 | 1.83 | 0.201 |
| 0.875 | 0.438 453 21 | 2.25 | 0.161 |
| 0.93 | 0.473 102 90 | 3.20 | 0.121 |

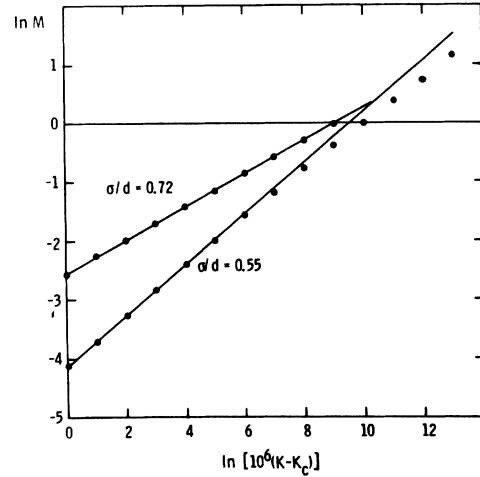


FIG. 8. Logarithm of the magnetization as a function of the logarithm of $[10^6(K - K_c)]$ for the two values of the parameter σ/d , 0.55 and 0.72. The lines are tangent to the curves at the end closest to K_c .

a couple values of σ/d are plotted in Figs. 8 and 9. We see from the figures that the exponents β and γ' can be determined quite accurately. The calculated values are plotted versus σ/d in Fig. 10. The exponent $\delta = (d + \sigma)/(d - \sigma)$ is related to β and γ' via the scaling relation

$$\delta = 1 + \gamma'/\beta.$$

The end points of the range $\sigma/d = 1$ and $\sigma/d = \frac{1}{2}$ de-

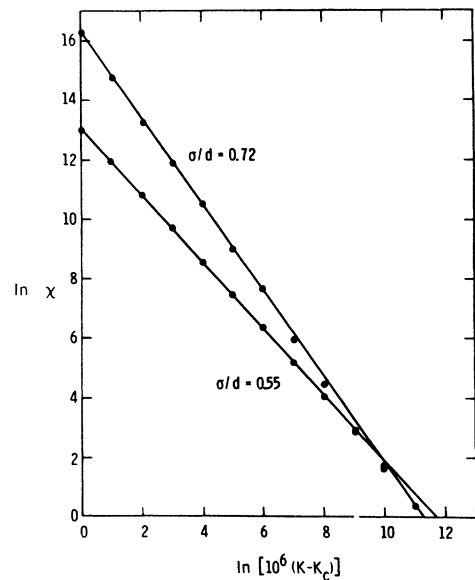


FIG. 9. Logarithm of the susceptibility as a function of the logarithm of $[10^6(K - K_c)]$ for the two values of the parameter σ/d , 0.55 and 0.72. The lines are tangent to the curves at the end closest to K_c .

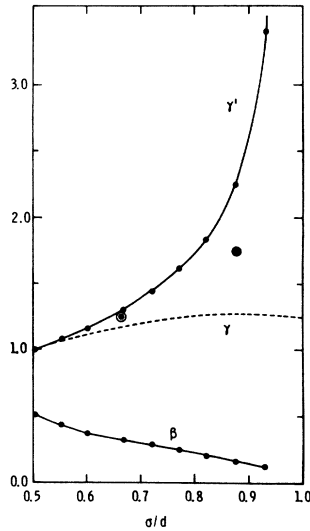


FIG. 10. The solid curves plot the critical indices γ' and β as a function of the parameter σ/d for the hierarchical model. The circled points give the known values of γ for the spin- $\frac{1}{2}$ Ising model in 3 and 2 dimensions, respectively. The dashed curve gives the index γ computed from the ϵ expansion carried to order ϵ^3 .

serve special mention, as these do not yield typical renormalization-group fixed-point behavior. As yet little is known about the case $\sigma/d=1$. Asymptotic analysis of the recursion formula for $\sigma/d < 1$, allows the determination of the large y behavior for the fixed-point function $Q^*(x)$ to be $Q^*(x) \sim x^{1+\delta}$. For $\sigma/d=1$, the exponent is infinite and asymptotic analysis would seem to indicate that a fixed point does not exist. It has also been noted in another context by Wilson and Kogut^{7,16} that, since for $\sigma/d=1$ the variable x is no longer rescaled upon each iteration of the recursion formula,

$$Q_{\mu+1}(x) = -2 \ln[I_\mu(x)/I_\mu(0)], \quad (3.13)$$

there may possibly no longer be universal behavior of the system after many iterations. This lack may result from the fact that the small x behavior of $Q_\mu(x)$ can no longer expand its influence with each iteration. Thus, the case $\sigma/d=1$, remains an open question and will not be discussed further here.

The case $\sigma/d=\frac{1}{2}$, has already received much attention. It is the point of bifurcation of non-Gaussian critical fixed-point solutions for $\sigma/d > \frac{1}{2}$ from the line of Gaussian critical fixed-point solutions for $0 < \sigma/d < \frac{1}{2}$, and its critical behavior is therefore characterized by Gaussian critical exponents modified by logarithmic corrections.

It is about the endpoint of the range $\sigma/d=\frac{1}{2}$ that the usual ϵ expansions are made, where $\epsilon = 4 - d$. Indeed, from the known series expansion for η

$= 2 - \sigma$ and γ we may write⁹

$$\begin{aligned} \sigma/d = (2 - 0.018\,518\,518\,5\epsilon^2 - 0.018\,689\,986\epsilon^3 \\ + 0.008\,328\epsilon^4 + \dots)/(4 - \epsilon) \end{aligned} \quad (3.14)$$

and

$$\gamma = 1 + \frac{1}{6}\epsilon + 0.077\,160\,494\epsilon^2 - 0.048\,970\epsilon^3 + \dots \quad (3.15)$$

for the $n=1$, (only one vector component) Landau-Ginzburg model. It is interesting to compare the hierarchical model results with those for the above ϵ expansion and with those for the $d=2$ and $d=3$ Ising model. This comparison is given in Fig. 10. It is further to be noted that the hierarchical model and the Wilson recursion relations for the same values ($d=3$, $\sigma=2$) of their parameters do not yield¹ the same value of γ ; thus for the model given by Eqs. (2.27) and (2.28) we expect γ to depend on more than the single parameter σ/d . Fig. 10 thus illustrates both the divergence of the ϵ expansion results from the Ising model results and the real difference between the short-range Ising model results and the intrinsically long-range hierarchical model results.

In Fig. 11, we show log-log plots of χ and M vs $(K_c - K)$ for $\sigma/d=\frac{1}{2}$. They clearly indicate a slowly varying correction to the dominant exponential behavior, which for Gaussian critical behavior is simply

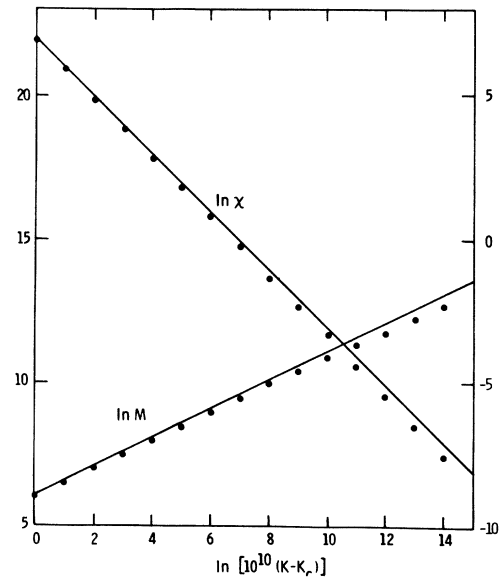


FIG. 11. Logarithm of the susceptibility and the magnetization for $\sigma/d=\frac{1}{2}$ plotted vs the logarithm of $[10^{10}(K - K_c)]$. The lines have the theoretical asymptotic slope and pass through the data point closest to K_c . The scale for the susceptibility is read to the left and magnetization to the right.

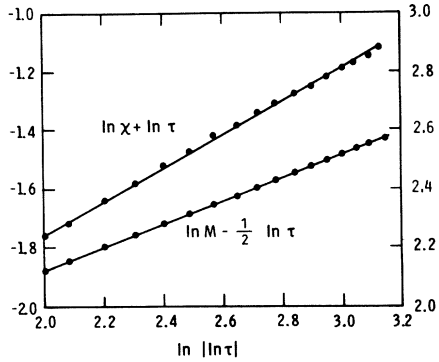


FIG. 12. Hierarchical model: plot of $\ln[\tau\chi]$ and $\ln[M\tau^{-1/2}]$ for $\sigma/d = \frac{1}{2}$ vs $\ln|\ln\tau|$. The lines show the best $|\ln\tau|$ to a power fits of $\tau\chi$ and $M\tau^{-1/2}$. The quantity $\tau = K - K_c$. The susceptibility curve scale is to the left, and that for magnetization to the right.

$$\begin{aligned} \chi &\sim |K - K_c|^{-1}, \\ M &\sim (K - K_c)^{1/2}, \quad K > K_c. \end{aligned} \quad (3.16)$$

Assuming that the dominant correction is logarithmic, we plot in Fig. 12 the quantities $\ln|(K - K_c)\chi|$ and $\ln|M/(K - K_c)^{1/2}|$ vs. $\ln|\ln|K - K_c||$. Within the indicated error over the range available, we may approximate the variation by a straight line. The apparent slopes are 0.56 for the susceptibility and 0.40 for the magnetization compared with the theoretical predictions of $\frac{1}{3}$ for each slope. By way of comparison, we have also studied the log corrections calculated from Wilson's recursion formulas ($b = 2$). The results are plotted in Fig. 13. The apparent slopes near $K - K_c = 10^{-6}$ have decreased markedly to 0.34 and 0.28 but still do not agree with the leading order

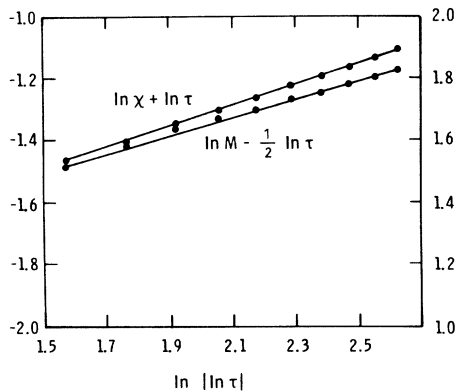


FIG. 13. Wilson's approximate recursion relation ($b = 2$): plot of $\ln[\tau\chi]$ and $\ln[M\tau^{-1/2}]$ for $\sigma/d = \frac{1}{2}$ vs $\ln|\ln\tau|$. The lines show the best $|\ln\tau|$ to a power fits of $\tau\chi$ and $M\tau^{-1/2}$. The quantity $\tau = K - K_c$. The susceptibility curve scale is to the left and that for magnetization to the right.

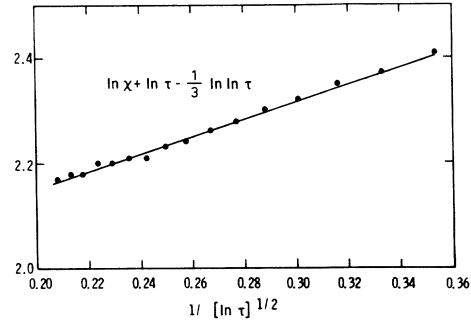


FIG. 14. Variation of the logarithm coefficient of the leading order term in the susceptibility for $\sigma/d = \frac{1}{2}$ (hierarchical model) plotted vs $[\ln\tau]^{-1/2}$. $\tau = K - K_c$.

predictions. The range over which our data (Fig. 12) runs is incomparably better than an experimentalist can hope to obtain, ranging from $K - K_c = 10^{-10}$ to 3×10^{-4} . We believe that this lack of agreement with theory is caused by the *very slow decay* of the subdominate terms. Since there is no reason to suppose that the amplitudes of these terms are in any way universal, the different apparent slopes become quite reasonable. To illustrate the possibility of the conformity of the theory with our results we have plotted in Fig. 14 the behavior of $\ln(\chi|K - K_c| |\ln|K - K_c||^{-1/3})$ vs $|\ln|K - K_c||^{-1/2}$. Over the range available, there is no problem in fitting the behavior with corrections of this sort. In the light of this analysis, it is quite plain that the experimental verification of $|\ln|^{1/3}$ type corrections is completely vain. That is not to say however, that a comparison of the full theoretical curve with relevant experimental data is without interest.

IV. NUMERICAL RESULTS NEAR THE TRICRITICAL POINT

By studying the behavior of the recursion formula for increasing values of the applied staggered field,

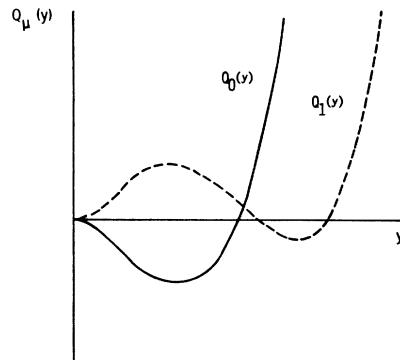


FIG. 15. Initial development of $Q_\mu(y)$ in the range of only moderate values of the staggered magnetic field.

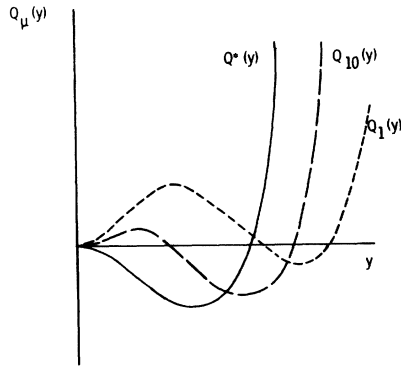


FIG. 16. Further development of $Q_\mu(y)$ for moderate values of the staggered magnetic field and $K=K_c(H')$.

crossover from a second-order to a first-order transition could be observed. For moderate values (i.e., still second order) of the staggered field the spin distribution function, after one iteration of the recursion formula, developed the form shown in Fig. 15. Clearly, $Q_1(y)$ now has the form of the continuous, spin-one, Ising distribution function discussed above at Eq. (2.24). If K is chosen at its critical value $K_c(H')$, the local maximum in $Q_\mu(y)$ becomes weaker upon successive iterations of the recursion formula, eventually converging to the zero-field, critical, fixed-point $Q^*(y)$ as shown in

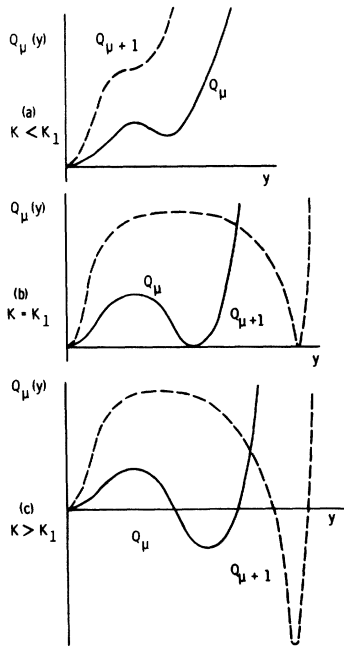


FIG. 17. Development of $Q_\mu(y)$, large μ , for larger values of the staggered magnetic field and (a) $K < K_1(H')$, the first order transition temperature, (b) $K=K_1$, and (c) $K > K_1$.

TABLE III. Tricritical points for the hierarchical model.

| σ/d | K_t | $(\sqrt{2} \bar{M}/J)H'_t$ |
|---------------|---------------|----------------------------|
| $\frac{3}{5}$ | 0.581 946 51 | 3.306 05 |
| $\frac{5}{3}$ | 0.643 809 691 | 3.428 14 |
| $\frac{7}{6}$ | 0.912 326 02 | 3.905 78 |

Fig. 16.

The dependence of the critical temperature on the value of the nonordering field was found, for small fields, to be $T_c(H') \propto H'^2$ as expected from Eq. (2.31). This can be compared with the Riedel-Wegner-Blum-Emery-Griffiths model where the dependence on the nonordering field was found to be $T_c(A') \propto A'$, as expected from Eq. (2.26).

As H' increases, the local maximum becomes stronger, with an increasing number of iterations being required before $Q_\mu(y)$ converges back to the fixed point $Q^*(y)$. Finally, for H' sufficiently large, the local maximum becomes dominant through successive iterations of the recursion formula and a fixed point no longer can be found. Instead a first-order transition is observed as illustrated in Figs. 17(a), 17(b), 17(c) for K less than, equal to, and greater than the first-order transition temperature $K_1(H')$. Thus at the transition temperature, the spin distribution function $e^{-Q_\mu(y)}$ acquires a new maximum corresponding to the appearance of a finite (rescaled) spontaneous magnetization. The width of the maximum decreases, as expected, with successive iterations of the recursion formula, indicating the vanishing of fluctuations as the system size grows beyond the correlation length.

At the boundary between the first- and second-order regions is found the tricritical fixed point, unstable in both temperature and nonordering field. For such doubly unstable fixed points, the bifurcation value of σ/d from Gaussian to non-Gaussian behavior is $\sigma/d = \frac{2}{3}$. Thus, we expect to obtain clas-

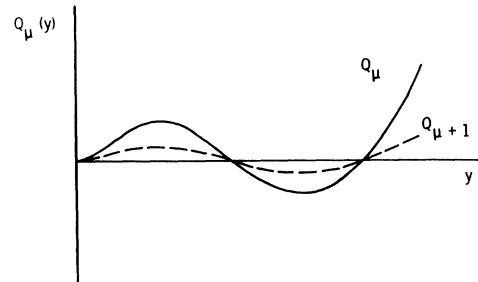


FIG. 18. The development of $Q_\mu(y)$, μ large, for $0 < \sigma/d \leq \frac{2}{3}$ at the tricritical point, $K=K_t$, $H'=H'_t$.

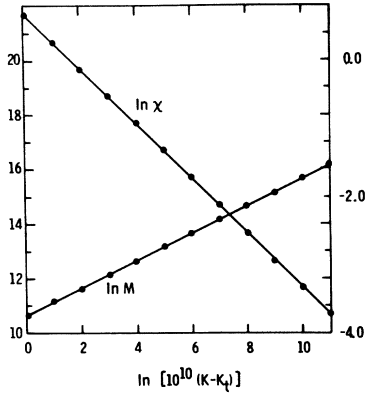


FIG. 19. Plot of the logarithm of the susceptibility and the magnetization for $\sigma/d=0.6$, $H' = H'_t$ vs the logarithm of $10^{10}(K-K_t)$. The scale for the susceptibility curve is to the left and that for the magnetization to the right.

sical tricritical exponents for $0 < \sigma/d < \frac{2}{3}$, nonclassical tricritical exponents for $\frac{2}{3} < \sigma/d < 1$, and classical exponents modified by logarithmic corrections for $\sigma/d = \frac{2}{3}$. The cases we have studied are $\sigma/d = \frac{3}{5}$, $\frac{2}{3}$, and $\frac{7}{8}$, which correspond to the values $d = 3\frac{1}{2}, \eta = 0$; $d = 3, \eta = 0$; and $d = 2, \eta = \frac{1}{4}$, respectively. The tricritical values K_t and H_t for the three choices of σ/d are presented in Table III. For $0 < \sigma/d \leq \frac{2}{3}$, the qualitative behavior of $Q_\mu(y)$ at the tricritical point $K = K_t, H' = H'_t$ is illustrated in Fig. 18. We see the function $Q_\mu(y)$ behaves as $f(\mu)Q_t(y)$ where $f(\mu) \rightarrow 0$ as $\mu \rightarrow \infty$. For $\sigma/d = \frac{2}{3}$, $f(\mu) \sim \mu^{-1}$ as $\mu \rightarrow \infty$, while for $0 < \sigma/d < \frac{2}{3}$, $f(\mu) \rightarrow 0$ exponentially fast. The function $Q_t(y)$ interpolates smoothly between second- and first-order behavior, and the local maximum is unstable to either growth or decay.

In Fig. 19, we plot our results for the magnet-

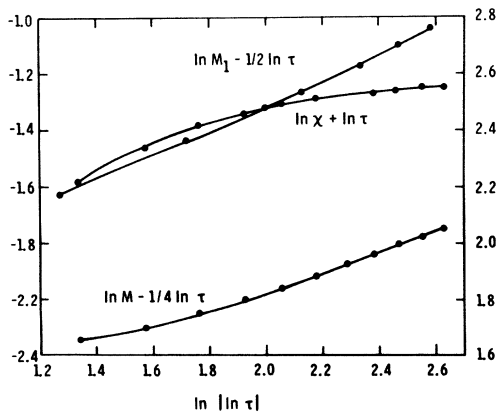


FIG. 20. Plot of $\ln(M_1 \tau^{-1/2})$, $\ln(\chi \tau)$ and $\ln(M \tau^{-1/4})$ for $\sigma/d = \frac{2}{3}$ vs $\ln |\ln \tau|$. The quantity $\tau = K - K_t$. The scale for the magnetization curves is to the right and that for the susceptibility curve to the left.

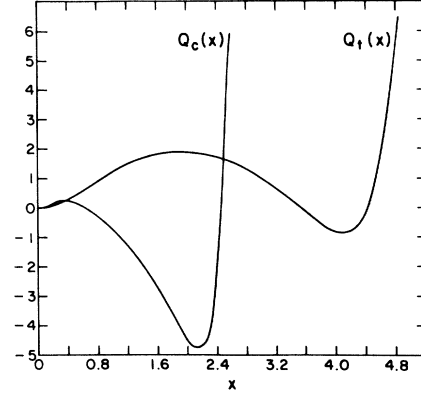


FIG. 21. Critical and tricritical fixed point functions $Q_c(x)$ and $Q_t(x)$ for $\sigma/d=0.875$.

ization and susceptibility calculations for $\sigma/d = \frac{3}{5}$, $H' = H'_t$ and $10^{-10} \leq |K - K_t| \leq 10^{-4}$. We have also computed $M_1(K_1)$, the spontaneous magnetization along the first-order line. We can thus also determine the critical exponent β_1 and the crossover exponent $\phi = \beta_t/\beta_1$. From these curves we determine the tricritical exponents $\gamma'_t = 1.00$, $\beta_t = 0.250$, $\beta_1 = 0.500 \pm 0.004$, and $\phi = 0.502 \pm 0.006$.

For $\sigma/d = \frac{2}{3}$ we therefore plot $\ln |\chi |K - K_t|$, $\ln |M_1/|K - K_t|^{1/2}|$, and $\ln |M/|K - K_t|^{1/4}|$ vs $\ln |\ln |K - K_t||$ in an attempt to determine the leading logarithmic corrections. This is done in Fig. 20.

In accordance with expectations [Eq.(2.34)] we observe no logarithmic corrections for χ . For M_1 and M_t we see the apparent behavior ($\tau = K - K_t$)

$$\begin{aligned} M_1 &\propto |\tau|^{1/2} |\ln |\tau||^x, \quad x = 0.46 \pm 0.04, \\ M_t &\propto |\tau|^{1/4} |\ln |\tau||^y, \quad y = 0.37 \pm 0.01, \end{aligned} \quad (4.1)$$

over our range $\tau = 10^{-10}$ to 10^{-1} (except 10^{-6} to 10^{-1} for M_t) instead of the expected values of $x = 0.7$, $y = 0.25$. Again, it is experimentally unfeasible to determine the exponents x and y in the face of subdominate, nonuniversal corrections which are only smaller by a factor of $|\ln |\tau||^{-1/2}$.

For the case $\sigma/d = \frac{7}{8}$, we have an example of a

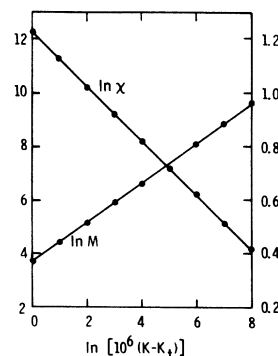


FIG. 22. Logarithm of the susceptibility and magnetization for H'_t and $\sigma/d=0.875$ vs the logarithm of $10^6(K-K_t)$.

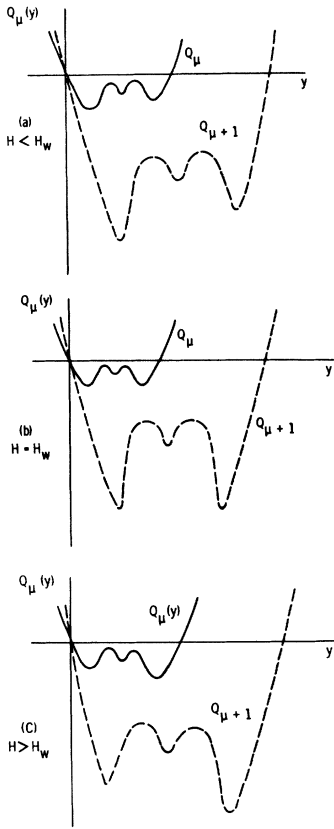


FIG. 23. Development of $Q_\mu(y)$ with μ large for $K = K_1(H')$, $H' > H'_t$ and (a) $H < H_w$, (b) $H = H_w$ and (c) $H > H_w$.

non-Gaussian tricritical fixed point. It is compared with the critical fixed point for $\sigma/d = \frac{7}{8}$ in Fig. 21. In Fig. 22, we plot our results for the magnetization and susceptibility calculated for $H' = H'_t$ over the range $10^{-6} \leq |K - K_t| \leq 1$. The resulting non-Gaussian tricritical exponents are found to be

$$\begin{aligned} \gamma'_t &= 1.03 \pm 0.02, & \beta_t &= 0.0737 \pm 0.0003, \\ \beta_1 &= 0.20 \pm 0.01, & \phi_t &= \beta_t/\beta_1 = 0.37 \pm 0.02. \end{aligned} \tag{4.2}$$

We next turn our attention to an attempt to see the wings associated with a tricritical point. By extending our model to the case $H \neq 0$, we are able

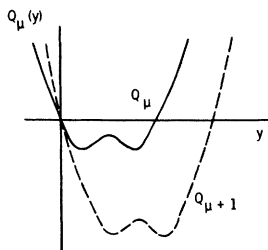


FIG. 24. Development of $Q_\mu(y)$ with μ large for a wing critical point.

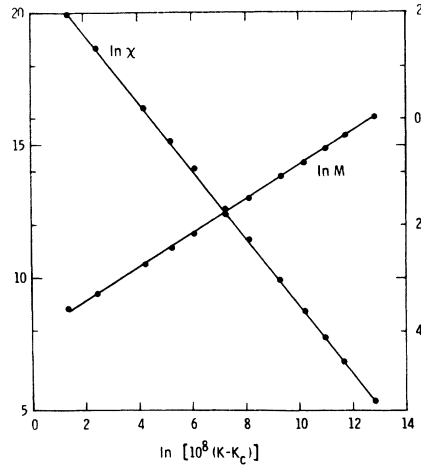


FIG. 25. Plot of the logarithm of the susceptibility and magnetization for $\sigma/d = \frac{2}{3}$ as a wing critical point is approached along the wing surface vs the logarithm of $10^8(K - K_c)$.

to study the full thermodynamic behavior in (H, H', T) space. In particular, we can study the wing coexistence surfaces, which extend out of the $H = 0$ plane, and determine the nature of the transition at the critical wing boundaries which extend from the tricritical point. We considered the case $\sigma/d = \frac{2}{3}$.

The wings location was determined in the following manner. We recall that the tricritical point was located at $(H_t = 0, H'_t = 3.428, K_t = 0.6438)$. First, the first-order transition temperature K_1 was determined for $H = 0, H' = 3.75$ to be $K_1 = 0.7789$. Then for fixed $H' = 3.80$ and $K = K_1(H' = 3.75)$, i.e., a point, for $H = 0$, between the wing surfaces, the ordering field H was varied to locate the surface of the wing. The wing surface could be recognized by the qualitative behavior of the spin distribution function $W_\mu(x)$ as a function of μ . This is indicated in Figs. 23(a)–23(c) where we show two successive iterations of $W_\mu(x)$, μ large, for values of H less than, equal to, and greater than the wing coexistence value H_w . We see in Figs. 23(a) and 23(c) that one or the other of two magnetization maxima dominate the spin distribution $e^{-(1/2)W_\mu(x)}$ depending on whether H is greater than or less than its wing coexistence value H_w , while in Fig. 23(b) for $H = H_w$ we see the coexistence of the two magnetization maxima having equal weight in the distribution function $e^{-(1/2)W_\mu(x)}$.

By varying H and K for fixed $H' = 3.80$, we could then move up the surface of the wing until the magnetization discontinuity across the surface vanished. This point defined a critical point on the wing boundary for

$$\begin{aligned} K_c(H' = 3.80) &= 0.731\ 29, \\ H_c(H' = 3.80) &= 0.080\ 679. \end{aligned} \tag{4.3}$$

The behavior of the critical function $Q_\mu(y)$ for two successive iterations of μ , μ large, is shown in Fig. 24. As a function of y it has the form of the ordinary critical fixed point function $Q^*(y)$, but is displaced along the y axis to correspond to the finite (rescaled) magnetization that exists at the wing boundary. This is as expected from universality.

As a final check on the Ising nature of the wing boundary critical points we calculated χ^* and M^* along the wing surface (both sides) to determine γ^* and β^* . The results are plotted in Fig. 25 from which we determine

$$\beta^* = \beta^- = 0.322 \pm 0.004, \quad \gamma^* = \gamma^- = 1.28 \pm 0.02, \quad (4.4)$$

consistent with the ordinary $\sigma/d = \frac{2}{3}$ critical point values.

ACKNOWLEDGMENTS

A conversation with R.B. Griffiths provided the starting point in our investigation of the wings. Thanks for helpful conversations are also due to M. Blume, V. Emery, M.E. Fisher, D. Furman, S. Krinsky, and E.K. Riedel.

*Work supported in part by U. S. ERDA, and in part by NSF Grant No. DMR76-01070.

¹G. A. Baker, Jr., Phys. Rev. B 5, 2622 (1972).

²G. A. Baker, Jr. and G. R. Golner, Phys. Rev. Lett. 31, 22 (1973).

³B. Simon and R. B. Griffiths, Commun. Math. Phys. 33, 145 (1973); Phys. Rev. Lett. 30, 931 (1973).

⁴E. K. Riedel and F. J. Wegner, Phys. Rev. Lett. 29, 349 (1972).

⁵F. J. Wegner and E. K. Riedel, Phys. Rev. B 7, 248 (1973).

⁶M. Blume, V. J. Emery and R. B. Griffiths, Phys. Rev. A 4, 1071 (1971).

⁷K.G. Wilson, Phys. Rev. B 4, 3184 (1971).

⁸K. G. Wilson and M. E. Fisher, Phys. Rev. Lett. 28, 240 (1972).

⁹E. Brézin, J. C. LeGuillou, and J. Zinn-Justin, in *Phase Transitions and Critical Phenomena*, Vol. 6, edited by C. Domb and M. S. Green (Academic, New York, 1977).

¹⁰D. S. Furman, Ph.D. thesis (State University of New York at Stony Brook, 1974) (unpublished).

¹¹A. L. Larkin and D. E. Khmel'nitskii, Zh. Eksp. Teor. Fiz. 56, 2087 (1969) [Sov. Phys.-JETP 29, 1123 (1969)].

¹²M. J. Stephen, E. Abrahams, and J. P. Straley, Phys. Rev. B 12, 256 (1975).

¹³G. R. Golner, Phys. Rev. B 8, 3419 (1973).

¹⁴*Handbook of Mathematical Functions*, edited by M. Abramowitz and I. A. Stegun (Dover, New York, 1965), p. 886.

¹⁵Reference 14, p. 879.

¹⁶K. G. Wilson and J. Kogut, Phys. Rep. C 12, 75 (1974).